Available online at www.sciencedirect.com
ScienceDirect
Journal of Nuclear Materials 367–370 (2007) 516–521
journal of nuclear materials
www.elsevier.com/locate/jnucmat

The influence of hydrogen on the fatigue behaviour of base and gas tungsten arc welded Eurofer

Marie-Françoise Maday *, Luciano Pilloni

ENEA-CR Casaccia, Via Anguillarese, 301, 00060 S. M. di Galeria, Rome, Italy

Abstract

Room temperature hydrogen embrittlement susceptibility of Eurofer base-metal and gas-tungsten-arc-welded joint has been investigated by fully-reversed load-control low cycle fatigue. The tests were run on specimens subjected to electrochemical charging before and during cyclic stressing. Compared to the uncharged condition, increasing amounts of hydrogen in base-steel caused fatigue life reduction by promoting premature cracking of either grain boundaries or cleavage planes. Examination of fracture morphologies indicated that the underlying embrittlement mechanisms likely correlated with plastic flow alteration and interatomic bond decohesion, both induced by hydrogen. Specimen-to-specimen response variability by test replication was accounted for in terms of Eurofer material heterogeneity, based on relevant experimental indexes. This interpretation was consistent with the well known sensitivity to microstructure of hydrogen embrittlement processes, and explained the large scatter of fatigue lives and failure modes subsequently observed in equivalently charged Eurofer weld samples.

1. Introduction

A 9Cr–1WTaV reduced activation ferritic/martensitic (RAFM) steel, Eurofer'97, is the reference structural material for the two EU concepts of DEMO blanket and for ITER Test Blanket Modules [1].

In the framework of the on-going R&D programme, characterization of out-of-pile microstructural and mechanical properties and behaviour under low-dose neutron irradiation of Eurofer'97 has almost been completed and the available results have been published [2]. Activities in progress are mainly focused at understanding the effect of high-level irradiation and in particular of helium production and He/dpa ratio at various temperatures and doses. The question of material embrittlement by hydrogen from transmutation reactions and other sources has long been speculated as being far less problematic and classified as second priority item, but this prediction might be non-conservative and the issue has been recently addressed.

In an earlier study [3], hydrogen embrittlement (HE) susceptibility of Eurofer'97 at room temperature (RT) was compared to that of conventional steels T91 and EM10 by means of tension tests run under electrochemical charging. Eurofer tensile

* Corresponding author. Tel.: +39 06 30484391; fax: +39 06 30483327.
E-mail address: francoise.maday@casaccia.enea.it (M.-F. Maday).

0022-3115/$ - see front matter © 2007 Elsevier B.V. All rights reserved.
doi:10.1016/j.jnucmat.2007.03.107

response to hydrogen was very scattered in replicated tests, and fell in between the fairly reproducible trends of the more (T91) and less (EM10) performing alloys. Based on other indexes, the main factors responsible for such variability (which may be inter-dependant) were grain boundaries (GB) for their irregular sizes, and Ta-oxides for their random distribution. Gaining additional evidence for a HE susceptibility/microstructure correlation was the objective of a continuing activity which was supported by the EU Structural Materials Programme 2004–2005 [4]. This paper describes part of this study, which was performed on Eurofer'97 base-steel and gas-tungsten-arc-welding (GTAW) joint by means of load-control low cycle fatigue (LCF) tests at RT and under hydrogen conditions properly selected from those previously employed.

2. Experimental

For the investigation, a $25 \times 400 \times 350$ mm plate of Eurofer heat E83694 produced by Bohler Edelstahl, GmbH, Austria was delivered in normalized and tempered (NT) condition (980 °C/30.6 min and 760 °C/90 min, air cooling). Nominal chemical composition in wt% is: 0.10%C, 0.050%Si, 0.45%Mn, 8.87%Cr, 1.15%W, 0.004%S, 0.005%P, 0.028%Ni, 0.20%V, 0.14%Ta, 0.005%Ti, 0.017%N, 0.08%Al. Cylindrical specimens with 10 mm gage length and 5 mm diameter were machined from the plate with their longitudinal axis parallel to rolling (TL specimen designation).

A Eurofer'97 butt-welded joint was prepared at CEA-Saclay, France by the multi-pass GTAW process on a $25 \times 500 \times 175$ mm plate of Eurofer heat E83694. A single V-groove (~16 mm top-gap; ~8 mm bottom gap), machined in the middle of the plate, was filled using Eurofer heat E83694 as the consumable. The welded assembly received a post-weld heat treatment (PWHT) of 750 °C/2 h at ENEA-Casaccia, Italy. Transverse cuts across the joint, sampling the molten zone (MZ), heat affected zone (HAZ), and adjacent base-metal (BM) were prepared for optical metallography, microhardness measurements, and precipitate size distribution evaluation which was performed on the digitalized scanning electron microscope (SEM, LEO 1530 FEG) images of the relevant weld regions, with image analysis software (AnalySIS Five, SEM version, Soft Imaging System GmbH). The LCF specimens were taken transverse to the weld so that their portion exposed to hydrogenation contained all zones of interest.

Each specimen, wrapped with Teflon tape except for the gage length, was fitted with an electrochemical cell and mounted on the load frame of a Instron testing machine (model 8862). Hydrogen charging was made at RT under galvanostatic control (EG&G, mod. 263A) with 4 mA/cm^2 applied current density to specimen immersed in either 0.1 M/l sodium hydroxide (referred to as condition 1) or in 0.1 M/l sulphuric acid with 3×10^{-5} M/l sodium arsenite as hydrogenation promoter (referred to as condition 2). The four-day precharging time which was used to ensure homogeneous distribution of dissolved hydrogen (referred to as saturation) throughout the 5 mm diameter gages before testing, was established in separate static experiments [4]. Charging was maintained to prevent hydrogen egress while running the fully-reversed load-control LCF experiments. Nominal stress amplitudes were in the range 407–484 MPa (0.72–$0.86\sigma_{0.2}$), and frequencies were either 0.03 and/or 0.1 Hz. Four to six replicated tests were conducted for each parameter combination, and continued to specimen rupture. Numbers of cycles to fracture, N_f, of charged versus uncharged samples were used to estimate the severity of HE through the fatigue life reduction factor given by

$$\mathrm{FR} = 100 \cdot (1 - N_f^{\mathrm{charged}}/N_f^{\mathrm{uncharged}}).$$

After testing, one specimen half was kept for fractographic examination under SEM, while the other half was immediately degreased, weighted, and transferred in a LECO analyzer. Hydrogen was extracted by thermal ramping from 400 °C to 1100 °C and at 50 °C/min and continuously measured by differential conductivity. Hydrogen concentration was calculated by normalizing the integrated flux to that of a standard.

3. Results and discussion

Microhardness measurements and optical metallography enabled discrimination of the main components of the weld joint (Fig. 1(a)). The MZ which was the hardest for the greatest content of un-precipitated carbon, consisted of tempered martensite lying inside a dendritic structure with large prior austenite grains, likely due to the lack of primary carbides. Adjacent HAZ was about 4 mm wide and comprised three distinct patterns: the region closest to fusion line, which certainly

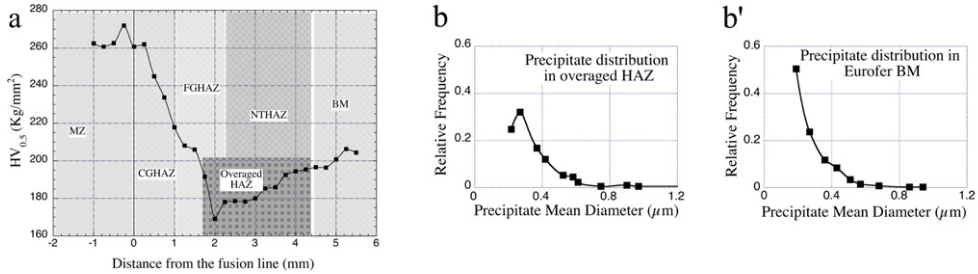

Fig. 1. (a) Vickers microhardness across welded joint. (b) Carbide distribution in overaged HAZ. (b′) Carbide distribution in BM.

experienced carbide dissolution, contained coarse grains (CG > 40 μm) as a result of their unrestricted growth. The next region was characterized by fine-grains (FG ~ 4–6 μm), presumably deriving from heating just above Ac_1 where recrystallization and grain refinement (or restricted grain growth) occurred due to undissolved carbides. The region towards the extreme edge of the HAZ consisted of NT martensite, virtually similar to BM (8–11 μm grain size), except for hardness. A comparative analysis of precipitate distribution versus size suggested that this latter region and part of the FGHAZ were softer likely due to carbide coarsening (Fig. 1(b) and (b′)) by over-tempering during welding and PWHT.

Hydrogen fluxes during thermal extraction from LCF specimens of either base or weld steel, exhibited broad and asymmetric profiles with a maximum around 560 °C. The representative trends in Fig. 2 showed that the peaks were far less resolved than in the tensile sample spectra recorded in previous work [3], which clearly highlighted the distinct peaks of hydrogen (H) release from trapping sites with increasing strengths. The variable relative heights of the first two signals in replicated extractions [3] were ascribed to a variable distribution on a sample scale of Ta-oxides and GB, based on microstructure observation. The impossibility of separating these signals in the LCF spectra likely arose from peak broadening, as a consequence of the larger test-piece diameter requiring a longer time for H extraction.

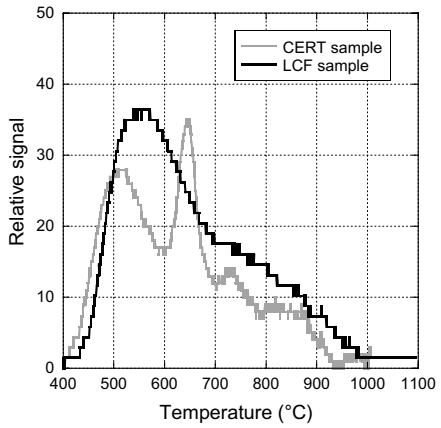

Fig. 2. Comparison of hydrogen extraction spectra from tensile and LCF samples.

Table 1 reports the fatigue live reduction factors, FR, of Eurofer base steel and weld from replicated tests as a function of nominal stress amplitude, frequency and average H concentrations [H], measured immediately after sample rupture. For comparison, the corresponding saturation concentrations $[H]_{sat}$ introduced by four-day precharging have been reported as average values of three extraction measurements. $[H]_{sat}$ represents the total H-solubility (in lattice and traps) at equilibrium with external H set by each charging condition, and uniformly distributed across specimen gage before testing.

$[H]_{sat}$ results on base-steel demonstrated the greater hydrogenation potentiality of condition 2 over condition 1, in conformity with the expected stimulating effect of H-adsorption promoter. Prediction that $[H]_{sat}$ should vary in proportion to trap density well complied with the lower values extracted from weld samples than from base-steel, since their exposed region mainly incorporated coarse grained zones (MZ and CGHAZ) and thus reduced fractional GB areas for collecting H. Based on the same prediction, it is likely that the higher H concentrations measured after ([H]) than before ($[H]_{sat}$) testing had a microstructural foundation. The origin might be the generation of additional traps during cycling, which captured hydrogen from the nearby lattice, so that a compensating H-flux was needed to replenish the lattice at its equilibrium coverage. The frequency-dependant character of

Table 1
LCF life reduction factors, FR%, of Eurofer as a function of LCF parameters and average hydrogen concentrations ([H] in wppm) calculated from extraction measurements on specimens after replicated LCF tests. ($[H]_{sat}$ are the average concentrations introduced by 4 day pre-charging at saturation just before testing and determined in separate tests)

Stress amplitude		$0.71\sigma_{0.2}$	$0.77\sigma_{0.2}$	$0.81\sigma_{0.2}$	$0.86\sigma_{0.2}$
Uncharged base-steel					
0.03 Hz	[H]	0.1	0.1	0.2 ± 0.1	0.2 ± 0.1
0.1 Hz	[H]		0.1		
Uncharged weld-joint					
0.03 Hz	[H]	0.3 ± 0.1	0.3 ± 0.1		
Base-steel – condition 1 ($[H]_{sat} = 2.2 \pm 0.2$)					
0.03 Hz	[H]		2.7 ± 0.2	2.4 ± 0.2	2.2 ± 0.2
	FR%		0	0	20
Base-steel – condition 2 ($[H]_{sat} = 5.5 \pm 0.2$)					
0.03 Hz	[H]	7 ± 0.3	6.6 ± 0.3		
	FR%	65–97	89–100		
0.1 Hz	[H]		6 ± 0.2		
	FR%		42		
Weld joint – condition 2 ($[H]_{sat} = 5 \pm 0.2$)					
0.03 Hz	[H]	5.7 ± 0.2	5.5 ± 0.2		
	FR%	MZ: 80 HAZ: 80–97	MZ: 80 HAZ: 80–90		

H-enrichment during the available testing time (around 59 000 s at 0.1 Hz and in between 700 and 34 000 s at 0.03 Hz [4]) suggested that the rate of extra H-supply was unlikely dictated by diffusion alone, but was aided by dislocation transport. The positive effect of decreasing frequency from 0.1 Hz to 0.03 Hz on H surplus also implied major dislocation efficacy for H-dragging and thus stronger H-dislocation interaction when frequency was lower, due to more suitable dislocation displacement rate.

Fatigue cracking of uncharged base-steel was of the ductile type and sequentially developed by nucleation at specimen periphery, stable propagation along striated plateaux till final instability by microvoid coalescence. Hydrogen impact on fatigue life reduction under charging condition 1 at 0.03 Hz was moderate since it required stress amplitude above $0.81\sigma_{0.2}$, and involved the intergranular (IG) decohesion of few grains of larger size ($\approx$30 μm) than the average (8–11 μm). Conversely, charging condition 2 was so detrimental that dramatic loss of fatigue performance ensued at lower stress amplitudes, but to different degree under test replication. Fractures were totally brittle and started by internal cracking, selectively running across the larger grains, and characterized by the cubic shapes of cleavage plane micro-bursts (referred to as micro-

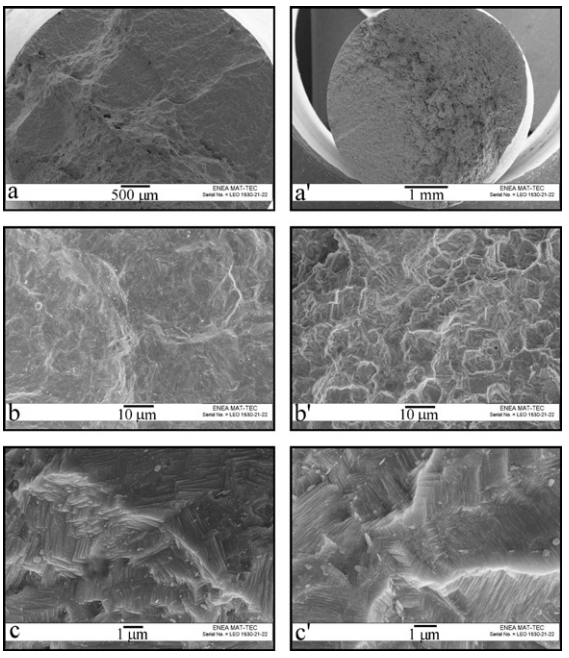

Fig. 3. Internal HE of base-steel under condition 2 charging at 0.03 Hz frequency: (a) fracture overview; (b) selective embrittlement of larger grained regions, (c) micro-cleavage facets. H-assisted cracking of base-steel under condition 2 charging at 0.1 Hz frequency: (a′) crack overview; (b′) unselective translath path; (c′) micro-cleavage facets.

cleavage) (Fig. 3(a)–(c)). At 0.1 Hz, the magnitude of H-damage and data scatter was comparatively far less pronounced. A single crack from the sample periphery propagated by translath micro-cleavage irrespective of grain size, and terminated by plastic instability (Fig. 3(a′)–(c′)).

Mechanical rupture of uncharged joint samples occurred across the overaged NTHAZ, as verified by optical metallography [4], and was morphologically similar to that of base-steel. Under condition 2 charging and 0.03 Hz, the fracture process zone was located alternatively in MZ or in the overaged NTHAZ. In the first case, fatigue lives were reproducible but significantly shorter compared to uncharged state. Cracks, with origin at sample periphery, grew across the lath packets by micro-cleavage before final collapse (Fig. 4(a)–(c)). In the second case, hydrogen caused drastic but variable drops of fatigue resistance from specimen-to-specimen. Internal and mixed transgranular/IG fracture appeared to be triggered by local micro-cleavage at coarse carbide/matrix interfaces (Fig. 4(a′)–(c′)).

Several indications given by these results support previous conclusions that HE mechanisms in Eurofer mainly correlated with both decohesion and dislocation (or plastic flow) theories [5].

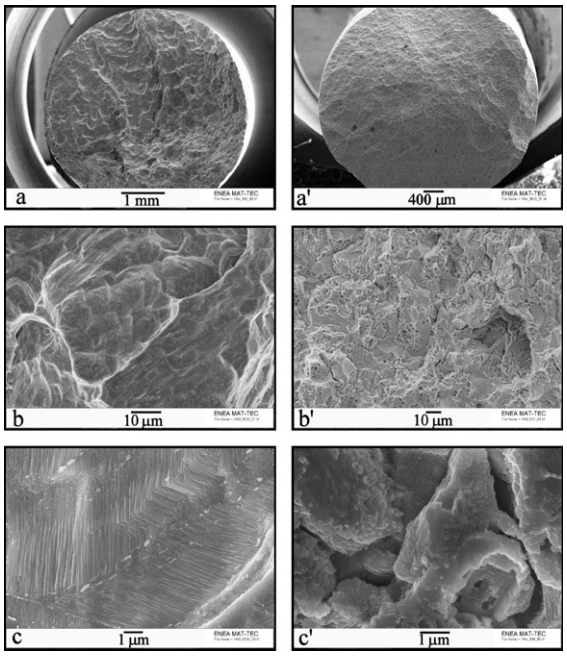

Fig. 4. H-assisted cracking in MZ of welded Eurofer: (a) crack overview; (b) translath path across elongated grains; (c) micro-cleavage facets. Internal HE of overaged NTHAZ: (a′) fracture overview; (b′) mixed IG/translath path; (c′) micro-cleavage around coarsened carbides.

For instance, IG cracking or micro-cleavage which respectively occurred alternatively under moderate or severe charging at the expense of the ductile path, testified that segregated hydrogen weakened the cohesive strengths of GB or cleavage planes, but in various proportion depending on the respective coverage.

Evidence of H effect on plastic flow was provided by the lack of deformation which accompanied fracture of base-steel and weld samples under condition 2 charging. Brittleness located everywhere or at specific singularities suggested that a H-blocking dislocation cross-slip mechanism was operative at obstacles so that additional accumulation of both pile-up stresses and hydrogen should be expected there.

The degenerative synergy between H-induced decohesion and interaction with dislocations could be inferred from the very premature fracture of base-steel when charging condition 2 and 0.03 Hz were used in combination. These parameters were so critical that micro-cleavage started internally before any surface crack had sufficient time to nucleate. Embrittled cleavage planes were those embodied in larger grains, presumably for their major H-enrichment, owing to the smaller GB fractional area involved in competitive H-capture than in finer grained regions. Since base-steel fatigue live reduction was also very scattered in replicated tests, it was likely that these lath packets had an unequal distribution from one specimen to another or needed variable incubation times to meet fracture criterion [6].

Internal embrittlement which did not manifest at 0.1 Hz during the time required for crack nucleation at sample periphery, probably suffered delay based on the above-mentioned prediction of weaker H-dislocation interaction at this frequency. It could be inferred that an unselective propagation to grain size ensued because hydrostatic stress elevation at the crack-tip was high enough to overcome the fracture stress of any cleavage plane regardless of its state of weakness. The typical insensitivity of surface crack initiation to internal heterogeneity combined with an undiscriminative crack propagation, could explain why the overall fracture kinetics were more reproducible than in the case of internal onset.

$[H]_{sat}$ reached under condition 1 appeared viable for base-steel, because cleavage planes were totally immune of HE, and because the few manifestations

of IG cracking not only required high applied stresses but also involved unsuitable grain sizes which could be avoided by proper metallurgical control.

HE behaviour of weld steel, even though not fully understood, was nonetheless of interest because it highlighted the importance of competitive trapping on H-damage [7].

Unlike base-steel, weld specimen fracture initiation was most likely controlled by the coarsened carbides lying in NTHAZ. These particles represented a new trap family, probably having higher binding energy for hydrogen and thus better trapping potentiality than their smaller precursors. Possibly, the achievement of a critical condition for fracture at previous susceptible cleavage planes was prevented or permanently delayed, for the beneficial H-dilution imparted by such concurrent carbides at their own expense. There was nonetheless evidence that carbide/matrix interfaces were more or less resistant against H-damage from one sample to another. This variability likely derived from microstructure heterogeneity of original base-steel, but the question as to which precise characteristics were beneficial or detrimental could not be answered from the present results. Certainly, unfavourable carbide configurations existed where interface decohesion started before crack initiation at free specimen surface. Whenever this occurred, FR results were scattered suggesting the existence of variable internal propensities. In the other case, surface cracks started in coincidence of hard MZ, unlike in H-free samples. In this case also, translath cleavage planes experiencing the high hydrostatic stress field, presumably failed without distinction (if any) because the associated fatigue life reduction was fairly reproducible, just like the global result of unresponsive processes to any eventual differences of internal susceptibility.

4. Conclusions

The results of this study and their interpretation allow formulation of the following conclusions:

Eurofer base-steel and welded joint were susceptible to HE under cyclic loading, as a consequence of atomic bond decohesion and stress accumulation processes.

The magnitude and manifestation of damage depended on H-concentration and on its interplay with microstructural and mechanical factors.

Internal HE phenomena were instances of extreme H-impact on steel performances, which imparted dramatic but quite scattered fatigue live reduction in replicated tests, as evidence of variable distribution of in-bulk susceptibility on a sample scale.

Cleavage planes inside larger grains than the average were the preferred sites for internal HE in base-steel, due to the poor competitive trapping of their surrounding. Such larger grains also were primarily responsible for crack growth enhancement due to embrittlement of their boundary at H concentration as low as 2 wppm.

The main deleterious factors for weld joint internal cracking were the coarsened carbides which developed in the HAZ during PWHT. Nonetheless, the more or less propensity of their interfaces to damage could not be actually explained, and needs more systematic investigation, perhaps on simulated HAZ microstructures.

Current understanding provided by this study, even though not exhaustive, is that HE problems in Eurofer might be mitigated by proper microstructural control.

References

[1] K. Lackner, R. Andreani, D. Campbel, et al., J. Nucl. Mater. 307–311 (2002) 993.
[2] A.A.-F. Tavassoli, A. Alamo, L. Bedel, et al., J. Nucl. Mater. 329–333 (2004) 257.
[3] M.F.Maday, L. Pilloni, in: Proceedings of the 20th IEEE/NPSS Symposium on Fusion Engineering, San Diego, CA, 14–17 October 2003, p. 185.
[4] M.F. Maday, L. Pilloni, EFDA Technology Workprogramme, Task TW3-TTMS003, Deliverable2, 2005.
[5] H.K Birnbaum, in: R.P. Gangloff, B. Ives (Eds.), Environmentally-Induced Cracking of Metals, NACE 10, Houston TX, 1990, p. 21.
[6] L. Coudreuse, J. Charles, Corros. Sci. 27 (1987) 1169.
[7] G.M. Pressouyre, I.M. Bernstein, Acta Metall. 27 (1979) 89.